



# Synthesis, characterization and performance of $\text{Cd}_{1-x}\text{In}_x\text{Te}$ compound for solar cell applications

Atef Y. Shenouda<sup>a,\*</sup>, Mohamed M. Rashad<sup>a</sup>, Lee Chow<sup>b</sup>

<sup>a</sup> Central Metallurgical R&D Institute (CMRDI), Tebbin, P.O. Box 87 Helwan, Cairo 11412, Egypt

<sup>b</sup> Department of Physics, University of Central Florida, Orlando, FL 32816, USA

## ARTICLE INFO

### Article history:

Received 16 October 2012

Received in revised form 12 February 2013

Accepted 13 February 2013

Available online 26 February 2013

### Keywords:

Cadmium indium telluride

Optical properties

Photo electrochemical cell

## ABSTRACT

$\text{Cd}_{1-x}\text{In}_x\text{Te}$  ( $x = 0.0, 0.2, 0.4, 0.6, 0.8$  and  $1.0$ ) samples have been synthesized chemically using wet chemical method from precursor compounds,  $\text{CdSO}_4$ ,  $\text{InCl}_3$ , and  $\text{TeCl}_4$ . The hydroxide form of the solution mixture was obtained by using ammonia solution and the pH of the mixture was adjusted to 9. A suitable amount of  $\text{NaBH}_4$  solution was added to reduce the hydroxide phase to the metalloid alloy. The crystal structure has been studied using powder X-ray diffraction (XRD) and scanning electron microscopy (SEM) measurements. The  $300^\circ\text{C}$  annealed samples revealed a cubic crystal structure. The morphology of the prepared samples is very fine and the average diameter is between 1 and  $2.5\ \mu\text{m}$ . The optical properties were determined using UV–vis–NIR spectrophotometer and band gap energy of 1.37 eV for  $\text{Cd}_{0.6}\text{In}_{0.4}\text{Te}$  was obtained. The best photovoltaic conversion efficiency of 1.89% was obtained for the  $\text{Cd}_{0.6}\text{In}_{0.4}\text{Te}$  sample with a short circuit current density ( $J_{sc}$ ) of  $15.3\ \text{mA cm}^{-2}$ , an open circuit voltage ( $V_{oc}$ ) of 0.668 V, and a filling factor (FF) of 69.31%.

© 2013 Elsevier B.V. All rights reserved.

## 1. Introduction

The growth of the high quality cadmium telluride ( $\text{CdTe}$ ) fine crystalline powder has been well-studied because of its potential applications in semiconducting devices, photovoltaic optoelectronic devices, radiation detectors, laser materials, thermoelectric devices, solar energy converters, Videocon devices, sensors, medical imaging and nanodevices [1–11].  $\text{CdTe}$  is an interesting material with technologically important physical properties, used to produce various high-performance electro-optical and infra red detectors. It has a direct band gap of 1.56 eV at room temperature, allowing direct transitions between the valence and conduction bands and allows efficient radiative transitions. There are continued interests in  $\text{CdTe}$  thin films due to interests in their photovoltaic properties, optical properties and also on their alloy's nanostructures [12–14]. Particularly, the recent surge of interests in using mercaptosuccinic acid (MSA) capped  $\text{CdTe}$  quantum dots as highly fluorescent sensor for biological applications, and as temperature sensor, or using mercaptopropionic acid (MPA) capped  $\text{CdTe}$  quantum dots as chemical sensor or as oxygen sensor [15–18]. Also, mechanical alloying for  $\text{CdTe}$  was reported [19].

Several ternary and quaternary semiconductors are currently investigated for their potential in photovoltaic applications [20,21]. The study of these materials is important due to the fact that the band gap and lattice parameters can be varied by changing

the cation composition.  $\text{CuInGaSe}_2$  (CIGS) chalcopyrite thin film absorber material is one of the most promising candidates for its high efficiency and low cost thin film solar cell. Recently, some II–III<sub>2</sub>–VI<sub>4</sub> ternary compounds such as  $\text{CdIn}_2\text{Te}_4$  have attracted attention both from fundamental and applied point of view.  $\text{CdIn}_2\text{Te}_4$  is a semiconducting compound with energy band gap 1.1 eV and its structure is basically a chalcopyrite structure with half of one of the cations removed [22]. Furthermore, a complete range of solid solution is possible in  $(\text{CdTe})_{1-x}(\text{In}_2\text{Te}_3)_x$  system for the compounds formed by mixing  $\text{CdTe}$  and  $\text{In}_2\text{Te}_3$ . Hence,  $\text{Cd–In–Te}$  offers a system in which the optical band gap could be varied in a wide range of interest. Indium is one of the interesting candidates as n-type dopants in  $\text{CdTe}$ . One of the methods for the incorporation of In atoms at low concentrations to  $\text{CdTe}$  has been achieved by co-evaporation of  $\text{CdTe}$  and metallic indium [23,24]. Therefore, the aim of this work is to improve the semiconducting properties of  $\text{CdTe}$  by indium addition. The change in the crystal structure, crystallite size and microstructure was investigated by using XRD analysis and SEM. Moreover, the optical properties were determined and the efficiencies of the photoelectrochemical cell by substitution of In ion were measured.

## 2. Experimental

### 2.1. Materials and methods

$\text{Cd}_{1-x}\text{In}_x\text{Te}$  (where;  $x = 0, 0.2, 0.4, 0.6, 0.8$  and  $1.0$ ) samples have been prepared chemically from stoichiometric ratios of  $\text{Cd}^{2+}$ ,  $\text{In}^{3+}$  and  $\text{Te}^{4+}$  using  $\text{CdSO}_4$ ,  $\text{InCl}_3$  and  $\text{TeCl}_4$  solutions, respectively. The pH solution was adjusted at 9 using ammonia

\* Corresponding author. Tel.: +20 2 25010640; fax: +20 2 25010639.

E-mail address: [ayshenouda@yahoo.com](mailto:ayshenouda@yahoo.com) (A.Y. Shenouda).

solution. Therefore, the hydroxide phase was precipitated. A suitable amount of  $\text{NaBH}_4$  solution was added to the mixture to reduce the hydroxide phase to the metalloid alloy. After that, the mixture was stirred with heating at around  $85^\circ\text{C}$  for 2 h. The solution mixture was left overnight to cool and precipitate the metalloid alloy compound by decantation. Then, the precipitant was filtered out and washed by 1% of  $\text{NaBH}_4$  solution followed by distilled water. Finally, the prepared powders were annealed at  $300^\circ\text{C}$  for 2 h in argon atmosphere.

## 2.2. Physical characterization

The crystalline phases were identified by X-ray diffraction (XRD) on a Bruker axis D8 diffractometer with crystallographic data software Topas 2 using  $\text{Cu K}\alpha$  ( $\lambda = 1.5406\text{ nm}$ ) radiation operating at 40 kV and 30 mA. The angle scan rate was set at  $2^\circ/\text{min}$ . The particles morphology was studied with a scanning electron microscope (JEOL, model JSM-5040). Elemental compositions of the various  $\text{Cd}_{1-x}\text{In}_x\text{Te}$  samples were analyzed by inductively coupled plasma (ICP, Perkin-Elmer Optima 2000 DV). The UV–vis transmission spectrum was measured by a UV–vis–NIR spectrophotometer (Jasco-V-570 spectrophotometer, Japan).

## 2.3. Electrochemical measurements

The electrochemical impedance spectra (EIS) measurements were carried out using cell holder of two electrodes. The samples powders were pressed into pellets of 12 mm diameter and 3 mm thickness. The amplitude was 20 mV and the frequencies varied from  $10^5\text{ Hz}$  to 10 mHz. For photo electrochemical cell, the working electrode prepared from  $\text{Cd}_{1-x}\text{In}_x\text{Te}$  sample materials was painted on conducting borosilicate glass substrate (dimensions:  $2.5\text{ cm} \times 1.1\text{ cm} \times 7\text{ cm}$ ) coated with a thin film of indium tin oxide (ITO). The conducting glass was purchased from SPI Company, USA.

The active area was  $2.5\text{ cm} \times 2.5\text{ cm}$ . Counter electrode was Pt. The cell configuration was fabricated: Glass/ITO/ $\text{Cd}_{1-x}\text{In}_x\text{Te}$ /0.5 M  $\text{Na}_2\text{S}$  + 0.5 M S + 0.5 M NaOH/Pt and characterized through current–voltage ( $I$ – $V$ ) measurements using silver halogen filament light source of 500 W [25]. The open circuit potential ( $V_{oc}$ ) and the short circuit currents ( $I_{sc}$ ) were recorded for the coated active material.

## 3. Results and discussion

The XRD patterns of the annealed  $\text{Cd}_{1-x}\text{In}_x\text{Te}$  ( $x = 0, 0.2, 0.4, 0.6, 0.8$  and  $1.0$ ) powder samples are shown in Fig. 1.  $\text{CdTe}$  and  $\text{Cd}_{0.8}\text{In}_{0.2}\text{Te}$  samples (samples “a and b”) display well defined XRD patterns with six diffraction peaks. These peaks are corresponded, respectively to the diffraction lines produced by the (111), (220), (311), (422) and (511) crystalline planes. The lattice parameter ‘a’ for cubic samples was calculated using the relation:  $a = d(h^2 + k^2 + l^2)^{0.5}$ , where  $h, k, l$  are the lattice planes and ‘d’ is the interplanar spacing, measured using Bragg’s equation. The obtained results for these samples are in agreement with cubic

**Table 1**  
Unit cell parameters for  $\text{Cd}_x\text{In}_{1-x}\text{Te}$  samples.

$\text{Cd}_x\text{In}_{1-x}\text{Te}$ samples	$a$ (Å)	$V$ (Å <sup>3</sup> )	$L$ (nm)
CdTe	6.51	275.98	22.97
$\text{Cd}_{0.8}\text{In}_{0.2}\text{Te}$	6.497	274.26	20.61
$\text{Cd}_{0.6}\text{In}_{0.4}\text{Te}$	6.483	272.56	18.60
$\text{Cd}_{0.4}\text{In}_{0.6}\text{Te}$	6.43	265.89	16.09
$\text{Cd}_{0.2}\text{In}_{0.8}\text{Te}$	6.313	251.65	15.25
InTe	6.101	227.1	18.08

structure of  $\text{CdTe}$  with space group  $Fm\bar{3}m$  [19]. Samples c, d, and e show more than one phase for  $\text{In}_2\text{Te}_3$ ,  $\text{InTe}$  and  $\text{CdIn}_2\text{Te}_4$  [26–28]. The obtained phase of  $\text{InTe}$  is cubic ( $Fm\bar{3}m$ ). The unit cell parameters are recorded in Table 1. It is observed that the lattice parameter “a” decreases by the increase of the indium substitution. This is due to the smaller ionic radius of  $\text{In}^{3+}$ , which is 9.2 nm while  $\text{Cd}^{2+}$  is 9.9 nm. Similar data were reported by Fata et al. [29]. The high reactivity of  $\text{In}$  with  $\text{Te}$  results in stronger bonding which helps in getting a highly crystalline structure. The crystallite size of the formed  $\text{Cd}_{1-x}\text{In}_x\text{Te}$  was determined from the most intense peaks for  $\text{Cd}_{1-x}\text{In}_x\text{Te}$  and  $\text{InTe}$  based on Debye–Scherrer equation [30,31]. It is observed that the crystallite size decreases by the indium substitution.

The surface morphology of annealed  $\text{Cd}_{1-x}\text{In}_x\text{Te}$  samples investigated by SEM is shown in Fig. 2. The SEM micrographs clearly show structure homogeneities and remarkably different morphologies for different values of  $x$  ( $x = 0, 0.2, 0.4, 0.6, 0.8$  and  $1.0$ ). It is observed that the particles have very fine morphology. The average diameter is about  $2\ \mu\text{m}$  for  $\text{Cd}_{0.2}\text{In}_{0.8}\text{Te}$  and  $\text{InTe}$ , while the average particle size of  $\text{Cd}_{0.6}\text{In}_{0.4}\text{Te}$  is about  $1\ \mu\text{m}$ .

The UV–Vis transmission spectra of  $\text{Cd}_{1-x}\text{In}_x\text{Te}$  are shown in Fig. 3. Mainly, the transmission spectra are occurred between wavelength range 675 and 800 nm for these samples. The spectrum of  $\text{Cd}_{0.6}\text{In}_{0.4}\text{Te}$  has maximum peak at wave length 800 nm.

The optical absorbance  $A$  and the optical the absorption coefficient “ $\alpha$ ” is give by the following relations [32,33]:

$$\text{Log}(1/T) = \alpha t \quad (1)$$

$$\text{The absorbance } A = \text{Log}(I^0/I) = \alpha t \quad (2)$$

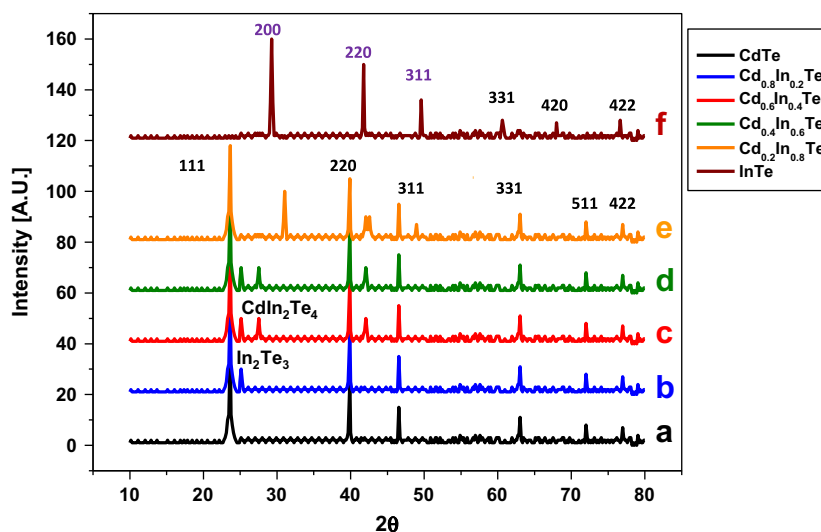


**Fig. 1.** XRD patterns of annealed compounds:  $\text{CdTe}$  (a),  $\text{Cd}_{0.8}\text{In}_{0.2}\text{Te}$  (b),  $\text{Cd}_{0.6}\text{In}_{0.4}\text{Te}$  (c),  $\text{Cd}_{0.4}\text{In}_{0.6}\text{Te}$  (d),  $\text{Cd}_{0.2}\text{In}_{0.8}\text{Te}$  (e) and  $\text{InTe}$  (f) at  $300^\circ\text{C}$  for 2 h in argon atmosphere.

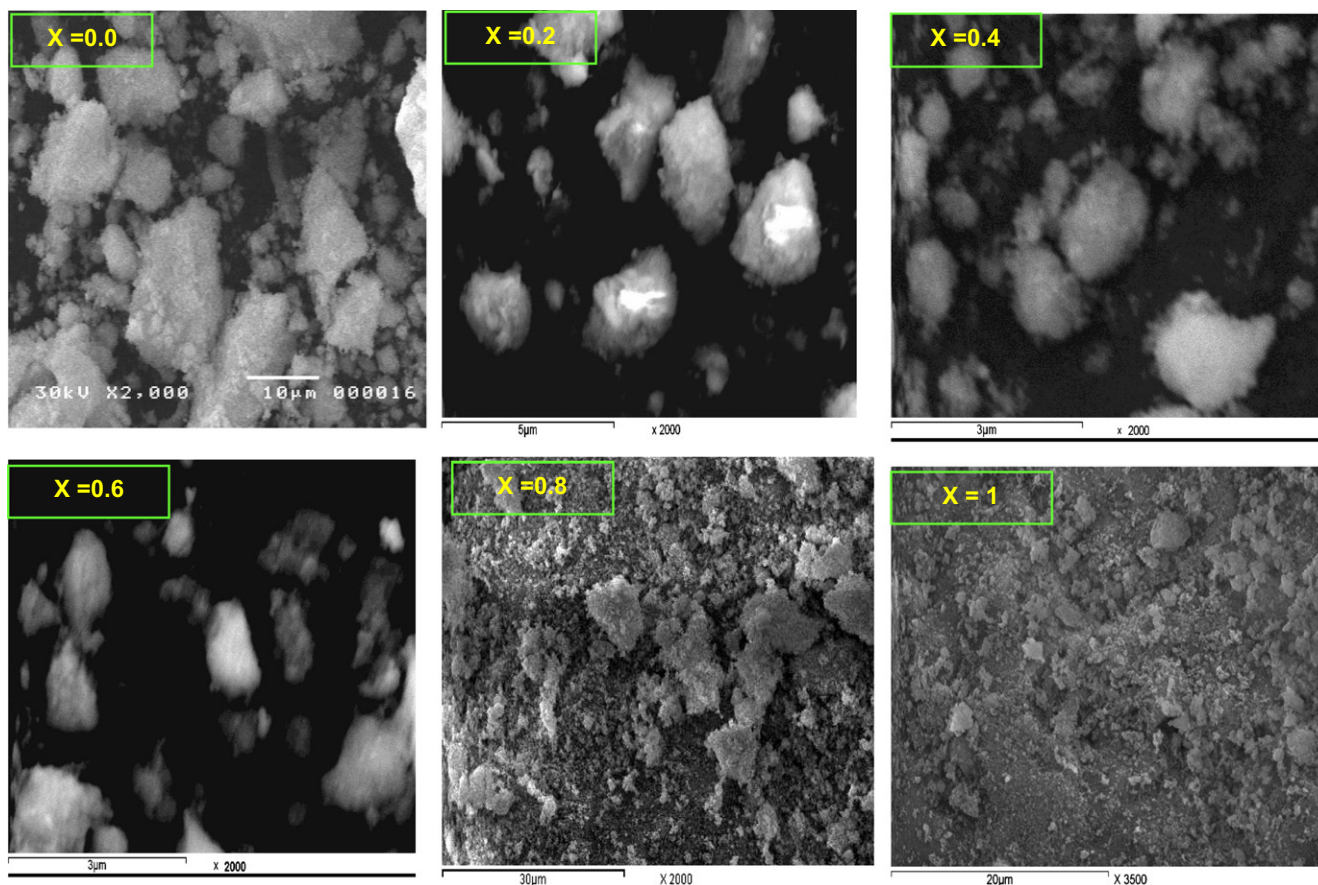


Fig. 2. SEM of  $\text{Cd}_{1-x}\text{In}_x\text{Te}$  ( $x = 0.0, 0.2, 0.4, 0.6, 0.8$  and  $1$ ) samples chemically prepared from Cd, In and Te ions solutions using  $\text{NH}_4\text{OH}$  and  $\text{NaBH}_4$ .

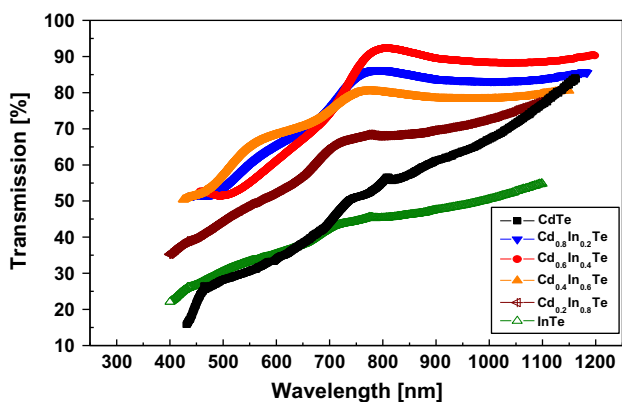


Fig. 3. Transmission spectra of  $\text{Cd}_{1-x}\text{In}_x\text{Te}$  ( $x = 0.0, 0.2, 0.4, 0.6, 0.8$  and  $1$ ) samples chemically prepared from Cd, In and Te ions solutions using  $\text{NH}_4\text{OH}$  and  $\text{NaBH}_4$ .

$$\text{Transmittance } \% T = 100(I/I^0) \quad (3)$$

where  $T$  is the transmittance of the spectra,  $t$  is the film thickness,  $I^0$  and  $I$  are the intensities of the incident and passed light through the sample. Analysis of optical absorption spectra is one of the most productive tools for determining optical band gap of the film.

From these spectral data, the absorption coefficient ( $\alpha$ ) for direct band semiconductors is given by:

$$\alpha h\nu = A(h\nu - E_g)^{0.5} \quad (4)$$

The relation between the direct transition  $(\alpha h\nu)^2$  and the absorption energy  $h\nu$  is plotted in Fig. 4.

The energy gap ( $E_g$ ) is determined by extrapolation. It is varied between 1.00 and 1.51 eV. The lowest  $E_g$ , 1.01 eV was achieved with  $\text{Cd}_{0.6}\text{In}_{0.4}\text{Te}$ . Therefore, the addition of In to substitute Cd metal seems to decrease the energy gap and facilitates the transition of electrons between the valence and conduction bands.

It was reported that the band gap energy of CdTe electrodeposited from the sulfate or chloride electrolyte was evaluated as 1.45–1.55 eV [34,35]. It was also reported by Garadkar et al. [36] that for CdTe powder synthesized by wet chemical route at pH 10.5 using  $\text{CdSO}_4$  and  $\text{Na}_2\text{TeSO}_3$  as starting materials, the energy gap values varied from 1.38 to 1.47 eV.

The EIS graph is given in Fig. 5. The values of the real impedance ( $Z'$ ) are  $1.14 \times 10^7$ ,  $5.6 \times 10^5$ ,  $1.18 \times 10^5$ ,  $1.24 \times 10^6$ ,  $1.05 \times 10^7$  and  $3.26 \times 10^7 \Omega$  for  $\text{Cd}_{1-x}\text{In}_x\text{Te}$  ( $x = 0, 0.2, 0.4, 0.6, 0.8$  and  $1.0$ ) samples, respectively. It is observed that  $\text{Cd}_{0.6}\text{In}_{0.4}\text{Te}$  and  $\text{Cd}_{0.8}\text{In}_{0.2}\text{Te}$  have the lower resistance ( $Z'$ ) in comparison with the other samples.

The  $I$ - $V$  curves as shown in Fig. 6 were further analyzed to evaluate power conversion efficiency ( $\eta$ ) and fill factor (FF%).

$$F = (V_{\max} I_{\max} / V_{\text{oc}} I_{\text{sc}}) \times 100\% \quad (5)$$

$$\eta = (V_{\max} I_{\max} / P_{\text{in}} \cdot A) \times 100\% \quad (6)$$

where  $V_{\text{oc}}$  is the open circuit potential for CdTe electrode,  $I_{\text{sc}}$  is the short circuit current measured at zero voltage,  $V_{\max}$  and  $I_{\max}$  are the optimum maximum voltage and current at the tangent point of the  $I$ - $V$  characteristic relation as observed in Fig. 5, and  $A$  is the working area of the active material electrode.

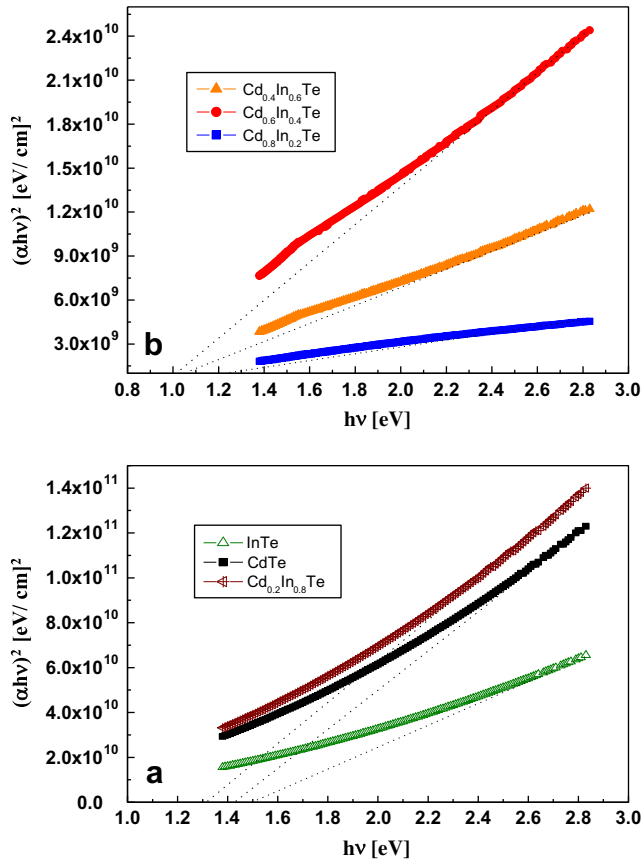


Fig. 4. Dependence of  $(\alpha hv)^2$  photon energy on  $h\nu$ , for Cd<sub>1-x</sub>In<sub>x</sub>Te (a) CdTe, InTe and Cd<sub>0.2</sub>In<sub>0.8</sub>Te; (b) Cd<sub>0.8</sub>In<sub>0.2</sub>Te, Cd<sub>0.6</sub>In<sub>0.4</sub>Te and Cd<sub>0.4</sub>In<sub>0.6</sub>Te samples.

The highest photo-conversion efficiency of 1.9% was achieved under simple laboratory conditions with Cd<sub>0.6</sub>In<sub>0.4</sub>Te as shown in Table 2. It was reported that CdTe/CdS solar cell gave an efficiency

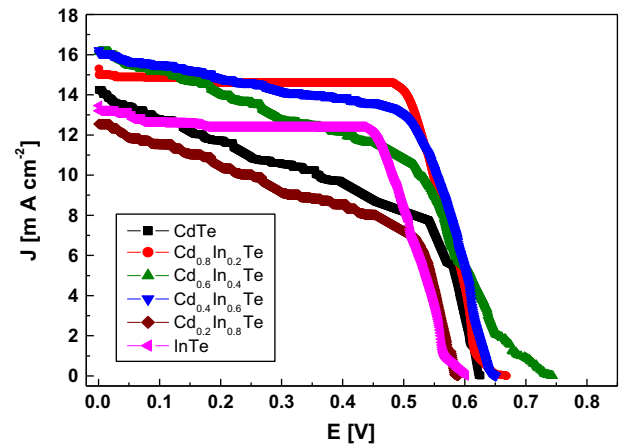


Fig. 6. Power output for the  $I$ - $V$  characteristics diagram of Cd<sub>1-x</sub>In<sub>x</sub>Te cells photoelectrochemical behavior.

Table 2  
Photo electrochemical cell (PEC) parameters for Cd<sub>x</sub>In<sub>1-x</sub>Te samples.

Cd <sub>x</sub> In <sub>1-x</sub> Te samples	$V_{oc}$ (V)	$I_{sc}$ (mA/cm <sup>2</sup> )	$V_{max}$ (V)	$I_{max}$ (mA/cm <sup>2</sup> )	FF (%)	$\eta$ (%)
CdTe	0.63	14.22	0.545	7.68	46.72	1.12
Cd <sub>0.8</sub> In <sub>0.2</sub> Te	0.65	16.24	0.450	13.09	55.80	1.57
Cd <sub>0.6</sub> In <sub>0.4</sub> Te	0.67	15.31	0.50	14.22	69.31	1.9
Cd <sub>0.4</sub> In <sub>0.6</sub> Te	0.61	13.49	0.45	12.26	44.17	1.43
Cd <sub>0.2</sub> In <sub>0.8</sub> Te	0.75	16.24	0.49	10.98	48.06	0.95
InTe	0.59	12.50	0.51	6.95	67.04	1.47

of about 0.89% on total area of flexible substrates [37,38]. Also, it was reported that the efficiency of electrodeposited CdSe was 0.34% [39]. Therefore, our results are considered promising in comparison with the reported ones.

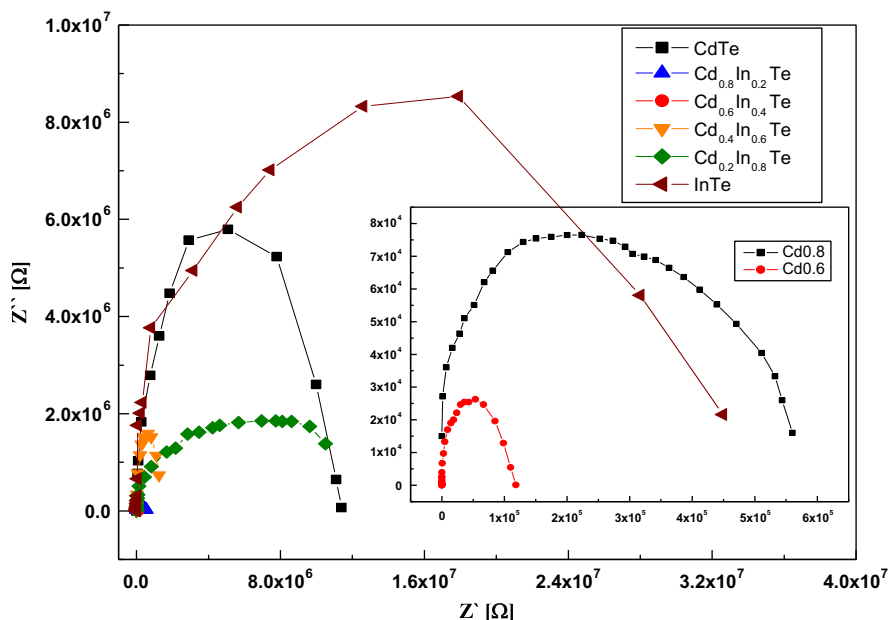


Fig. 5. EIS of Cd<sub>1-x</sub>In<sub>x</sub>Te ( $x = 0.0, 0.2, 0.4, 0.6, 0.8$  and  $1$ ) powder samples.

#### 4. Conclusions

The effect of In doping on CdTe have been studied. Cd<sub>1-x</sub>In<sub>x</sub>Te ( $x = 0, 0.2, 0.4, 0.6, 0.8$  and  $1.0$ ) samples were prepared chemically from stoichiometric ratios of Cd<sup>2+</sup>, In<sup>3+</sup> and Te<sup>4+</sup> using CdSO<sub>4</sub>, InCl<sub>3</sub> and TeCl<sub>4</sub> solutions, respectively. The pH value of the solution was adjusted at 9 using ammonia solution. A suitable amount of NaBH<sub>4</sub> solution was added to the mixture to reduce the hydroxide phase to the metalloid alloy. The energy gap ( $E_g$ ) varied between 1.0 and 1.5 eV. The lowest  $E_g$ , 1.01 eV was achieved with Cd<sub>0.6</sub>In<sub>0.4</sub>Te. The highest photovoltaic response was achieved by a power conversion efficiency of 1.9% with Cd<sub>0.6</sub>In<sub>0.4</sub>Te with  $J_{sc}$  of 15.3 mA cm<sup>-2</sup>,  $V_{oc}$  of 0.67 V and 69.31% FF.

#### Acknowledgment

The authors would like to offer their thanks to the Science and Technology Development Funds (STDF) for supporting this work through the fund of US–Egypt joint project no. 420.

#### References

- [1] J. Han, C. Liao, T. Jiang, C. Spanheimer, G. Haindl, G. Fu, V. Krishnakumar, K. Zhao, A. Klein, W. Jaegermann, *J. Alloys Comp.* 509 (2011) 5285–5289.
- [2] E.R. Shaaban, N. Afify, A. El-Taher, *J. Alloys Comp.* 482 (2009) 400–404.
- [3] U. Alver, E. Bacaksiz, E. Yanmaz, *J. Alloys Comp.* 456 (2008) 6–9.
- [4] R. Chandramohan, T. Mahalingam, J.P. Chu, P.J. Sebastian, *Sol. Energy Mater. Sol. Cells* 81 (2004) 371.
- [5] S.K. Deshmukh, A.V. Kokate, D.J. Sathe, *Mater. Sci. Eng. B* 122 (2005) 206.
- [6] J. Hu, T.W. Odom, C.M. Lieber, *Acc. Chem. Res.* 32 (1999) 435.
- [7] Y. Xia, P. Yang, Y. Sun, Y. Wu, B. Mayers, B. Gates, Y. Yin, F. Kim, H. Yan, *Adv. Mater.* 15 (2003) 353.
- [8] X. Duan, Y. Huang, R. Agarwal, C.M. Lieber, *Nature* 421 (2003) 241.
- [9] M. Gratzel, *Nature* 414 (2001) 338.
- [10] W.U. Huynh, J.J. Dittmer, A.P. Alivisatos, *Science* 295 (2002) 2425.
- [11] Robert. Triboulet, *J. Alloys Comp.* 371 (2004) 67–71.
- [12] R.K. Katiyar, S. Sahoo, A.P.S. Gaur, A. Singh, G. Morell, R.S. Katiyar, *J. Alloys Comp.* 509 (2011) 10003–10006.
- [13] E.R. Shaaban, N. Afify, A. Ei-Taher, *J. Alloys Comp.* 482 (2009) 400–404.
- [14] E. Yilmaz, E. Tugay, Aliyekber, I. Yildiz, M. Parlak, R. Turan, *J. Alloys Comp.* 545 (2012) 90–98.
- [15] Y. Zhu, Z. Li, M. Chen, H.M. Cooper, G.Q. Lu, Z.P. Xu, *J. Colloid Interface Sci.* 390 (2013) 3–10.
- [16] R. Liang, R. Tian, W. Shi, Z. Liu, D. Yan, M. Wei, D.G. Evans, X. Duan, *Chem. Commun.* 49 (2013) 969–971.
- [17] R.Q. Aucelio, A.I. Perez-Cordores, J.L.X. Lima, H.B.B. Ferreira, A.M.E. Guas, A.R.D. Silva, *Spectrochim. Acta A* 100 (2013) 155–160.
- [18] P.C. Lau, R.A. Norwood, M. Mansuripur, N. Peyghambarian, *Nanotechnol.* 24 (2013) 0155011–0155018.
- [19] C.E.M. Campos, K. Ersching, J.C. de Lima, T.A. Grandi, H. Höhn, P.S. Pizani, *J. Alloys Comp.* 466 (2008) 80–86.
- [20] H.J. Wu, S.W. Chen, T. Ikeda, G.J. Snyder, *Acta Mater.* 60 (2012) 1129–1138.
- [21] S. Perit, Th. Hoche, J. Dadda, E. Muller, P.B. Pereira, R. Hermann, M. Sarahan, E. Pippel, R. Brydson, *J. Solid State Chem.* 193 (2012) 58–63.
- [22] Kiran. Jain, R.K. Sharma, Sandeep. Kohli, K.N. Sood, A.C. Rastogi, *Curr. Appl. Phys.* 3 (2003) 251–256.
- [23] M.F. Cabrera, J. Dong, O.F. Sankey, *Thin Solid Films* 373 (2000) 19.
- [24] Ki.-Ho. Song, Seung.-Cheol. Beak, Hyun.-Yong. Lee, *J. Appl. Phys.* 108 (024506) (2010) 1–6.
- [25] A.V. Kokate, M.R. Asabe, S.D. Delekar, L.V. Gavali, I.S. Mulla, P.P. Hankare, B.K. Chougule, *J. Phys. Chem. Solids* 67 (2006) 2331–2336.
- [26] Z. Sztuba, K. Wiglusz, I. Much, A. Sroka, W. Gawel, *Calphad* 32 (2008) 106–110.
- [27] T. Suriwong, K. Kurosaki, S. Thongtem, A. Harnwungmoung, T. Plirdpring, T. Sugahara, Y. Ohishi, H. Muta, S. Yamanaka, *J. Alloys Comp.* 509 (2011) 7484–7487.
- [28] K. Yvon, W. Jeitschko, E. Parthe, *J. Appl. Cryst.* 10 (1977) 73.
- [29] F.L. Fanta, C.E.M. Campos, K. Ersching, P.S. Pizani, *Mater. Chem. Phys.* 125 (2011) 257–262.
- [30] Atef Y. Shenouda, Hua Kun. Liu, *J. Electrochem. Soc.* 157 (2010) A1183–A1187.
- [31] A.V. Kokate, M.R. Asabe, P.P. Hankare, B.K. Chougule, *J. Phys. Chem. Solids* 68 (2007) 53–58.
- [32] H. Khallaf, G. Chai, O. Lupan, H. Heinrich, S. Park, A. Schulte, Lee. Chow, *J. Phys. D: Appl. Phys.* 42 (2009) 135304.
- [33] R.M. Oksuzoglu, P. Bilgic, M. Yildirim, O. Deniz, *Opt. Laser Technol.* 48 (2013) 102–109.
- [34] K. Arai, K. Murase, T. Hirato, Y. Awakura, *J. Electrochem. Soc.* 152 (2005) C237–C242.
- [35] K. Arai, K. Murase, T. Hirato, Y. Awakura, *J. Electrochem. Soc.* 153 (2006) C121–C126.
- [36] K.M. Garadkar, S.J. Pawar, P.P. Hankare, A.A. Patil, *J. Alloys Comp.* 491 (2010) 77–80.
- [37] X. Mathew, J.P. Enriquez, A. Romeo, A.N. Tiwari, *Sol. Energy* 77 (2004) 831–838.
- [38] K.W. Mitchell, C. Eberspacher, F. Cohen, J. Avery, G. Duran, W. Bottenberg, *Sol. Cells* 23 (1988) 49–57.
- [39] S.M. Pawar, A.V. Moholkar, K.Y. Rajpure, C.H. Bhosale, *Appl. Surf. Sci.* 253 (2007) 7313–7317.